

Astrophysical Reaction Rates for $^{10}\text{B}(p,\alpha)^7\text{Be}$ and $^{11}\text{B}(p,\alpha)^8\text{Be}$ From a Direct Model

T. Rauscher

Institut für Kernchemie, Universität Mainz, Germany

and

*Institut für theoretische Physik, Universität Basel, Switzerland **

G. Raimann

Department of Physics, The Ohio State University, Columbus, OH, USA

Abstract

The reactions $^{10}\text{B}(p,\alpha)^7\text{Be}$ and $^{11}\text{B}(p,\alpha)^8\text{Be}$ are studied at thermonuclear energies using DWBA calculations. For both reactions, transitions to the ground states and first excited states are investigated. In the case of $^{10}\text{B}(p,\alpha)^7\text{Be}$, a resonance at $E_{Res} = 10$ keV can be consistently described in the potential model, thereby allowing the extension of the astrophysical S -factor data to very low energies. Strong interference with a resonance at about $E_{Res} = 550$ keV require a Breit-Wigner description of that resonance and the introduction of an interference term for the reaction $^{10}\text{B}(p,\alpha_1)^7\text{Be}^*$. Two isospin $T = 1$ resonances (at $E_{Res1} = 149$ keV and $E_{Res2} = 619$ keV) observed in the $^{11}\text{B}+p$ reactions necessitate Breit-Wigner resonance and interference terms to fit the data of the $^{11}\text{B}(p,\alpha)^8\text{Be}$ reaction. S -factors and thermonuclear reaction rates are given for each reaction. The present calculation is the first consistent parametrization for the transition to the ground states and first excited states

*current address

at low energies.

25.40.Hs, 24.10.Eq, 24.50.+g, 28.52.Cx

I. INTRODUCTION

The determination of the astrophysical S -factor of the reaction $^{10}\text{B}(p,\alpha)^7\text{Be}$ at thermonuclear energies is important in several respects. In the search for advanced fusion reaction fuels the reaction $^{11}\text{B} + p \rightarrow ^8\text{Be} + \alpha \rightarrow 3\alpha$ is discussed as a promising candidate for a relatively clean fusion fuel [1,2]. However, natural boron contains 19.7% ^{10}B which produces ^7Be contaminations via the $^{10}\text{B}(p,\alpha)^7\text{Be}$ reaction. Therefore, for a full understanding of the feasibility of boron as a fusion fuel one has to consider the rate for the latter reaction as well [3].

The importance of the $^{10}\text{B}(p,\alpha)^7\text{Be}$ reaction in astrophysical scenarios results from the fact that it is the dominant process for the destruction of ^{10}B . It was also claimed that it could be usefully incorporated in explaining the abundances of boron isotopes including the present theory of spallative generation of l elements [4,5]. Furthermore, in theoretical investigations of primordial abundances of elements, its rate has to be incorporated in the reaction networks employed in nucleosynthesis calculations for inhomogeneous big bang scenarios [6,7].

Experimental results for the $^{10}\text{B}(p,\alpha)^7\text{Be}$ reaction at energies below 1 MeV are scarce. There have been measurements of the $^{10}\text{B}(p,\alpha_0)^7\text{Be}$ cross sections with sometimes inconsistent results in the energy ranges $220 \text{ keV} < E_p < 480 \text{ keV}$ [8], $60 \text{ keV} < E_p < 180 \text{ keV}$ [9], $70 \text{ keV} < E_p < 205 \text{ keV}$ [10], and, more recently, $120 \text{ keV} < E_p < 480 \text{ keV}$ [4]. However, these measurements do not extend very far into the region dominated by the $J^\pi=5/2^+$ resonance ($E_x = 8.701 \text{ MeV}$ in ^{11}C [11]) which is of great importance for astrophysics. In our calculations we therefore focused on the description of the resonance and the reproduction of most recent data [12,13,14] at very low energies. The only available data measuring the α_1 contribution to the S -factor are given in Ref. [15].

The reaction $^{11}\text{B}(p,\alpha)^8\text{Be}$ has been measured below 1 MeV [16], [17], and most recently [14]. It should be noted that the effect of electron screening [14] increases the very low energy cross sections considerably and thus has a major impact on a reaction's significance as a terrestrial fusion fuel.

II. METHOD

It is commonly accepted that nuclear reactions for energies above about 20 MeV mainly proceed via a direct mechanism. For intermediate energies, however, distinct levels of the compound system are populated, resulting in many cases in pronounced resonances in the excitation functions. For astrophysically relevant energies, typically sub-Coulomb energies of a few keV or tens of keV, compound mechanisms are often very important. However, direct transitions can also be important at stellar energies. For example, the reactions of the pp-chains in the Sun are known to be mainly dominated by such direct mechanisms [18,19]. Recent theoretical investigations of a number of sub-Coulomb transfer reactions [20,21,22,23,24] have also shown that they can be described by a direct reaction potential model like the distorted wave Born approximation (DWBA). Although “direct reaction” is often used synonymously with “non-resonant”, the same potentials that describe the direct mechanism can give rise to resonances corresponding to energy levels in the projectile-target system. Such potential resonances are very broad at energies above the Coulomb barrier and do not alter cross sections significantly within several keV (or even a few MeV). However, due to the Coulomb barrier they become small at low energies, with typical widths of a few keV. A DWBA description of a resonance structure at thermonuclear energies of a three-nucleon transfer reaction is given in [24]. In the sub-Coulomb energy range of (p, α) reactions the DWBA method has previously only been used to analyze non-resonant parts of the excitation functions [21,22]. We want to emphasize, though, that it is possible to reproduce resonance features in a DWBA calculation.

For the results in this paper we utilized the zero-range DWBA code TETRA [25]. The differential cross section for the transfer reaction $a + A \rightarrow b + B$ with $a - x = b$, $A + x = B$ (stripping) using light projectiles and ejectiles (for $a \leq 4$ and $x = 1$ or $x = 3$) is given in zero-range DWBA by [26,27]

$$\frac{d\sigma}{d\Omega} = \frac{\mu_\alpha \mu_\beta}{(2\pi\hbar^2)^2} \frac{k_\beta}{k_\alpha} \frac{2J_B + 1}{2J_A + 1} \sum_{\ell s j} C^2 \mathcal{S}_{\ell j} N \frac{\sigma_{\ell s j}(\vartheta)}{2s + 1} \quad (1)$$

with the usual zero-range normalization constant $N = 1/2 aD_0^2 = 5.12 \cdot 10^5$ [28]. The spectroscopic factors $\mathcal{S}_{\ell j}$ relevant for our calculations were taken from [29].

Important for the success of our potential model is the fact that the input data for the optical potentials can be taken from realistic models, i.e. from semimicroscopic or microscopic formalisms such as the folding-potential model, the Resonating Group Method (RGM), or the Generator Coordinate Method (GCM). In this respect the potential model combines the first-principle approach of a microscopic theory with the flexibility of a phenomenological method.

In this work we used the method of the folding potential [23,30] to obtain the optical potentials in the entrance and exit channel as well as the potential for the bound state. The folding potential is given by [23]

$$U_F(\mathbf{r}) = \lambda \int d\mathbf{r}_A \int d\mathbf{r}_a \rho_A(\mathbf{r}_A) \rho_a(\mathbf{r}_a) V(E, \rho_A, \rho_a, s = |\mathbf{r} + \mathbf{r}_a - \mathbf{r}_A|) \quad . \quad (2)$$

In this expression \mathbf{r} is the separation of the centers of mass of the two nuclei in the channel, ρ_a and ρ_A are the respective nucleon densities and λ is the adjustable strength factor. The factor λ differs slightly from the value of 1 because it accounts for the effects of antisymmetrization and the Pauli principle. The effective NN interaction V for the folding procedure was of the DDM3Y type [31] and the density distributions were taken from Ref. [32] unless noted otherwise. For the bound state potentials λ is fixed, since the known binding energy of the transferred particle x , a triton, in ^{10}B or ^{11}B , respectively, has to be reproduced.

While the resonant cross section (or S -factor) of $^{10}\text{B}(p, \alpha_0)^7\text{Be}$ can be reproduced well by the DWBA alone, an interfering resonance in $^{10}\text{B}(p, \alpha_1)^7\text{Be}^*$ and – due to their unnatural parity – the resonances in $^{11}\text{B}(p, \alpha)^8\text{Be}$ have to be treated explicitly assuming, e.g., single-level Breit-Wigner expressions (see Sect. III.B).

III. RESULTS FOR $^{10}\text{B}(\text{p},\alpha)^7\text{Be}$

A. The Reaction $^{10}\text{B}(\text{p},\alpha_0)^7\text{Be}$

At high energies the transition to the ground state of ^7Be ($Q = 1.15$ MeV [33], binding energy $E_{bind} = 18.67$ MeV [34] of the triton in the ^{10}B nucleus) was previously analyzed by means of the DWBA method [35]. For the transition to the first excited state at sub-Coulomb energies, there has only been a simplified DWBA calculation of the direct reaction contribution to the cross section which considered only the Coulomb potential [36]. To our knowledge, no calculation of the contribution of the transition to the ground state at sub-Coulomb energies has been performed so far.

The spectroscopic factors $\mathcal{S}_{\ell j}$ are listed in Table I. For the calculation of the folding potential in the α - ^7Be channel as well as for the bound state ($\text{t-}^7\text{Be}$) the density distribution of ^7Li [32] was used instead of the unknown distribution of ^7Be .

In our calculation, the strength factor λ for the optical potential in the proton channel was adjusted in such a way that the phase shift of the optical s-wave at the resonance energy $E_{Res} = 0.01$ MeV was $\pi/2$, thereby producing the s-wave resonance previously suggested [4]. The value of λ in the alpha channel remained an open parameter since there are no elastic scattering data available for the unstable nucleus ^7Be . The imaginary part of the potential in the proton channel is very small because there are no other channels open at these low energies besides the (p,γ) and (p,α) channels. The complete set of optical parameters is given in Table II.

For the transition to the first excited state of $^7\text{Be}^*$ ($Q = 0.72$ MeV) the optical potential in the proton channel stays the same as for the ground state transition. We also assume that the potential for $^7\text{Be}^* + \alpha_1$ can, to first order, be approximated by the potential for $^7\text{Be} + \alpha_0$.

For $^{10}\text{B}(\text{p},\alpha_0)^7\text{Be}$ the resulting S -factors in the energy range $E_{c.m.} \leq 150$ keV are shown in Figs. 1 and 2. The experimental results [14] are well reproduced with the resonance width

being about 15 keV, in agreement with other measurements [11,33]. It should be noted that the calculated energy dependence of the S -factor is only valid for bare nuclei. Due to electron screening, measurements to even lower energies would not show the same Breit-Wigner like shape. The deviation of the experimental data at the two lowest measured energies in Fig. 1 is already due to screening effects [14]. The calculated differential cross sections show the same isotropic behaviour as can be seen in the data of Ref. [13].

B. The Reaction $^{10}\text{B}(\text{p},\alpha_1)^7\text{Be}^*$

Using the same approach as described above we also calculated the cross sections for the transition to the first excited state at energies $E_{c.m.} \leq 150$ keV. Interference effects with other resonances (especially a broad $5/2^+$ level at about 550 keV) were reported in [11] at slightly higher projectile energies. In order to successfully reproduce the experimental data [15] while keeping unchanged all of the parameters entering the DWBA computation, we had to include that $5/2^+$ level in our calculation. This was achieved by a single-level Breit-Wigner fit to the level at 550 keV and by finally calculating a total cross section (or S -factor, respectively) from the interference of the Breit-Wigner and the DWBA contributions.

The single level Breit-Wigner formula is given by [37]

$$\sigma(E) = \pi\lambda^2 \frac{2J_R + 1}{(2J_p + 1)(2J_B + 1)} \times \frac{\Gamma_p(E)_l \Gamma_\alpha}{(E - E_R)^2 + (\Gamma_{tot}(E)/2)^2} \quad . \quad (3)$$

The quantities J_R , J_p and J_B denote the total angular momentum of the resonance, of the incoming proton and of the ^{10}B target nucleus, respectively, $\Gamma_p(E)_l$ is the energy dependent proton partial width of the resonance with orbital angular momentum l , Γ_α is the energy independent alpha partial width, and $\Gamma_{tot}(E)$ is the total width of the resonance as given by

$$\Gamma_{tot}(E) = \Gamma_p(E)_l + \Gamma_\alpha \quad . \quad (4)$$

Γ_γ would be small and is neglected here. Due to the positive Q -value it is sufficient to consider the energy dependence of only the proton partial width Γ_p . This energy dependence can be described by [37]:

$$\Gamma_p(E)_l = \frac{2\hbar}{R_n} \left(\frac{2E}{\mu} \right)^{1/2} P_l(E, R_n) \theta_l^2 \quad , \quad (5)$$

with the penetrability

$$P_l(E, R_n) = \frac{1}{F(E, R_n)^2 + G(E, R_n)^2} \quad (6)$$

given in terms of the regular and irregular Coulomb wave functions F and G and the nuclear radius R_n . For simplicity, R_n will be derived here from the Coulomb charge radius (light ion convention):

$$R_n = r_c A_B^{1/3} \quad . \quad (7)$$

The dimensionless quantity θ_l is the reduced proton width.

The available experimental data [11,15] were not sufficient to yield an unambiguous fit within our calculation. A small alpha width leads to a larger proton width and vice versa. For example, with a resonance energy of $E_{Res} = 560$ keV we obtain the following pairs of alpha partial width and proton reduced width: $\Gamma_\alpha=0.1$ keV, $\theta_l=0.49$ and $\Gamma_\alpha=500.0$ keV, $\theta_l=0.01$. We were not able to distinguish between the different sets in our chi square fit. (However, the resonant (p, γ) cross section [11] seems to favor a large reduced width for the proton channel if the gamma width is assumed to be small).

Finally, we can write the energy-dependent S -factor as

$$S_{tot,\alpha_1}(E) = S_{DWBA}(E) + S_{BW}(E) - 2[S_{DWBA}(E)S_{BW}(E)]^{1/2} \cos \delta \quad . \quad (8)$$

The phase shift δ is given by [38]

$$\delta = \arctan \left(\frac{2(E - E_R)}{\Gamma_{tot}(E)} \right) - \frac{\pi}{2} \quad . \quad (9)$$

The total S -factors and the DWBA and Breit-Wigner contributions are shown in Fig. 3. Although the experimental data [15] are quite well reproduced at higher energies, the agreement slightly worsens toward lower energies. The experiment seems to give a larger value for the width of the 10 keV resonance. This is caused by the assumption that the imaginary

part of the optical potential in the proton channel is the same as for the transition to the ground state of ${}^7\text{Be}$. Actually, the imaginary part for the α_1 transition should be slightly larger because more flux is going into the α_0 channel than into the relatively small α_1 channel which is included in the imaginary part used for the ground state transition. With a larger imaginary part the resonance width is increased. This result is very sensitive to the depth of the imaginary optical potential; with an increase by only 50 keV the resonance structure is already flattened out completely. However, in order to get an upper limit on the contribution of this transition to the total S -factor we used the same optical potential as for the ground state transition.

The thermonuclear reaction rate $N_A \langle \sigma v \rangle$ is given in Table VI, where N_A is the Avogadro constant and the bracketed quantity is the velocity averaged product of the cross section and the relative velocity of the interacting particles [37]. In Fig. 4 the ratio of the resulting rate at low temperatures to the rate given in Ref. [39] is shown. This rate remained unchanged in a more recent compilation [40] of reaction rates. Since the $E_{Res} = 0.01$ MeV resonance was not taken into account in [39], its rates differ considerably from our new values in the corresponding temperature region. Our calculation shows that the contribution of the reaction ${}^{10}\text{B}(p, \alpha_1){}^7\text{Be}^*$ is less than 10^{-3} of the rate for the ground state transition, and that the compiled rates have to be revised.

IV. THE REACTIONS ${}^{11}\text{B}(p, \alpha_0){}^8\text{Be}$ AND ${}^{11}\text{B}(p, \alpha_1){}^8\text{Be}^*$

A. Available data

Cross sections for this reaction were measured in Ref. [17] (α_0 as well as α_1) and recently to even lower energies in Ref. [14] (sum of α_0 and α_1). In the latter case, the α_0 S -factor amounted to only about 1% of the α_1 value at energies below 500 keV. The reaction can proceed either via a direct 3α -breakup, or via a sequential decay involving the states of ${}^8\text{Be}$. It was demonstrated in [17] that the direct 3α -breakup makes no significant contribution

(less than 5 %) to the total cross section at all the energies investigated ($E_{c.m.} = 22$ to 1100 keV). It is therefore justified to describe the reaction in terms of a quasi-stable ${}^8\text{Be}$ nucleus interacting with an α -particle.

The S -factor of ${}^{11}\text{B}(p,\alpha_1){}^8\text{Be}^*$ is dominated by two $T = 1$ resonances at $E_{c.m.} = 149$ keV ($J^\pi = 2^+$, orbital angular momentum $l_R = 1$) and at $E_{c.m.} = 619$ keV ($J^\pi = 2^-$, $l_R = 0$) [33] in the ${}^{12}\text{C}$ compound system. Due to its unnatural parity, the $E_{c.m.} = 619$ keV resonance would not be expected to contribute to the S -factor of the ${}^{11}\text{B}(p,\alpha_0){}^8\text{Be}$ reaction. In Ref. [33] the two resonances are quoted as pure $T = 1$. Without at least a small admixture of $T = 0$, however, these resonances could not decay into the ${}^8\text{Be} + \alpha$ channel. The concept of isospin mixing has been thoroughly investigated and understood for the 1^+ states; experiments with pion scattering [41,42] show that several excited ${}^{12}\text{C}$ states exhibit quite considerable mixing. The two states in question would only be weakly excited in pion scattering and have not been observed, but it is plausible that all high-lying ${}^{12}\text{C}$ states are isospin mixed [43].

Within the simple approach adopted here, the DWBA calculation ($T = 0$) gives the non-resonant contribution. The mostly $T = 1$ resonances are reproduced by single-level Breit-Wigner terms, and the $T = 0$ admixture of the 619 keV resonance ($l_R = 0$) interferes with the mostly $l = 0$ direct part. The isospin mixing is accounted for implicitly in the Breit-Wigner approach via the decay width into the α -channel.

Lacking an appropriate representation for the direct contribution, Ref. [17] gives only a polynomial fit of the S -factor. In Ref. [14], the direct, non-resonant contribution is assumed to be energy independent, and the same formalism of a Breit-Wigner term plus an interference term is employed to describe the cross section. In this work, the determination of the direct contribution is based on a more basic calculation and the transition to the ground state is described with the same set of parameters.

B. The Calculation

The Q -value of this process is $Q = 8.59$ MeV [33], and the binding energy is $E_{bind} = 11.22$ MeV [34]; the spectroscopic factors \mathcal{S}_{ℓ_j} [29] including all constants are listed in Table III.

The calculation was performed using a ^8Be density distribution that was chosen [44] so that folding it with the triton density would reproduce the ^{11}B distribution. The strength parameter $\lambda_\alpha = 1.21$ is fairly close to the preliminary result obtained for the triple-alpha reaction [44].

The strength factor λ_p in the proton channel was kept as a free parameter, since there are no low energy elastic scattering data available suited for an optical potential fit. Differential cross sections measured at one angle [17] confirm that elastic scattering below 400 keV in the center-of-mass is consistent with the Rutherford scattering law.

Due to the low energy in the proton channel both the imaginary potential and a real spin-orbit term can be neglected. In the alpha channel, a non-zero Saxon-Woods imaginary part was used (the geometry parameters were roughly averaged between those for α - ^7Li and α - ^9Be , both taken from Ref. [45]). The complete set of optical parameters is given in Table IV. In first order, the optical potentials are assumed to be identical for the reactions to the ^8Be ground state and to the first excited state.

Similarly to the approach for $^{10}\text{B}(p,\alpha_1)^7\text{Be}^*$, a sum of Breit-Wigner terms and an interference term was used. The total S -factor for the reaction to the first excited state of $^8\text{Be}^*$ consists of the contributions by both resonances ($S_{Res1}(E)$ and $S_{Res2}(E)$ at $E_{c.m.} = 149$ keV and $E_{c.m.} = 619$ keV, with orbital angular momenta $l_R = 1$ and $l_R = 0$, respectively), the non-resonant contribution S_{NR} as calculated by the DWBA, and an interference term [14,38]:

$$S_{tot,\alpha_1}(E) = S_{Res1}(E) + S_{Res2}(E) + S_{NR}(E) - 2[S_{NR}(E)S_{Res2}(E)]^{1/2} \cos \delta \quad . \quad (10)$$

Each resonance is described by a single-level Breit-Wigner term (Eq. 3) with a fixed α -partial width Γ_α and an energy dependent proton partial width $\Gamma_p(E)$ expressed in terms of the

penetrability $P_l(E)$ and the reduced proton width θ_p . The phase shift δ is given by Eq. 9. The interference term is between the non-resonant component and the $T = 0$ fraction of the 619 keV resonance which is determined by the Breit-Wigner fit. There is no interference with the 149 keV resonance since it has $l_R = 1$.

The total S -factor for the reaction to the ^8Be ground state consists of only the S -factor contributions of the lower-energy resonance ($l_R = 1$) and the non-resonant term as calculated by the DWBA.

For a value of λ_p almost identical to the one used for $^{10}\text{B}(p,\alpha)^7\text{Be}$, the Breit-Wigner terms (including the energy dependent proton partial width) were fitted to the experimental data of Refs. [14] and [17]. The values of θ_p , Γ_α and E_{Res2} resulting from the fit are listed in Table V.

C. Results

The resulting S -factor curves are shown in Fig. 5. The dashed lines represent the non-resonant contribution of the DWBA, while the full lines include the Breit-Wigner resonances. In the absence of an interference term for the reaction to the ^8Be ground state, the DWBA alone reproduces the trend of the data points outside the resonance region. For the reaction to the first excited state of ^8Be , the DWBA curve is in good overall agreement with the ad-hoc assumption of a direct, non-resonant contribution made in Ref. [14], with the exception of a decrease of S_{NR} with increasing energy. Note the pronounced enhancement of the low energy data points due to the effect of electron screening [14].

Due to the strong contribution of interference effects to the α_1 S -factor, one cannot hope to describe the angular distributions with the DWBA. For the α_0 S -factor, however, such a description seems to be reasonable outside the resonance. In Ref. [14] no differential cross sections were measured. In Ref. [17] a few angular distribution curves are available, but they tend to disagree with measurements presently carried out [46]. The DWBA calculations favour Ref. [46], but the exact shape of the angular distributions depend crucially on the

value λ_p of the proton- ^{11}B folding potential.

The reaction rate $N_A \langle \sigma v \rangle$ of $^{11}\text{B}(\text{p},\alpha_1)^8\text{Be}^*$ is listed in Table VII and compared to the values obtained from the parametrization given in Ref. [40] (here, the contribution of the reaction $^{11}\text{B}(\text{p},\alpha_0)^8\text{Be}$ is neglected since it is about 10^{-2} of the rate for the transition to the first excited state). There is a slight enhancement of the rate at low temperatures due to the better description of the resonances and the direct contribution.

V. CONCLUSION

The reactions $^{10}\text{B}(\text{p},\alpha)^7\text{Be}$ and $^{11}\text{B}(\text{p},\alpha)^8\text{Be}$ are described well by the DWBA calculations. In the case of $^{10}\text{B}(\text{p},\alpha_0)^7\text{Be}$, we were able to reproduce the resonance structure in a consistent way within our potential model thus suggesting that it can be regarded as a potential resonance. The influence of the resonance on the reaction rate can be seen very clearly in Fig. 4 (a fairly constant S -factor was assumed in Ref. [40] at low energies). This clearly demonstrates that extrapolations from higher energies have to be done very carefully to include the correct shape of the resonance.

For the transition to the first excited state in ^7Be the interference effects with a $5/2^+$ level at about 550 keV have to be taken into account. This was achieved by including a Breit-Wigner term describing the resonance at 550 keV and an interference term between the DWBA and Breit-Wigner contributions. However, the cross sections of the α_1 transition are lower by several orders of magnitude than those of the α_0 transition and therefore it does not contribute significantly to the final reaction rate.

In the case of $^{11}\text{B}(\text{p},\alpha)^8\text{Be}$ the inclusion of an interference term between single-level Breit-Wigner and DWBA also reproduces the data acceptably well. Systematic studies at higher energies are being carried out at present [44].

ACKNOWLEDGMENTS

We want to thank G. Staudt and H. Oberhummer for discussions and comments on the manuscript, C. Angulo, F. Knape, and F.-K. Thielemann for discussions, and H. Clement for pointing out the results of pion scattering experiments. Our thanks also go to O. Schönfeld who supplied the α - ^8Be potential and to R.N. Boyd and M.J. Balbes for helpful comments on the manuscript and critical discussions. GR wishes to express his thanks to C. Rolfs for support during his stay in Münster and Bochum. This research was supported in part by the Deutsche Forschungsgemeinschaft (projects Ro429/18-2 and Ro429/21-3). TR acknowledges support by the Alexander von Humboldt foundation and by an APART fellowship of the Austrian Academy of Sciences. GR was supported by an Ohio State University postdoctoral fellowship.

REFERENCES

- [1] J. Raeder *et al.*, *Kontrollierte Kernfusion* (Teubner, Stuttgart, 1981).
- [2] R. Feldbacher and M. Heindler, *Nucl. Instr. Meth.* **A271**, 55 (1988).
- [3] R.J. Peterson, C.S. Zaidins, M.J. Fritts, N.A. Roughton, and C.J. Hansen, *Ann. Nucl. Energy* **2**, 503 (1975).
- [4] M. Youn, H.T. Chung, J.C. Kim, H.C. Bhang, and K.-H. Chung, *Nucl. Phys.* **A533**, 321 (1991).
- [5] H. Reeves, *Nuclear Reactions in Stellar Surfaces and Their Relations with Stellar Evolution* (Gordon and Breach, London, 1971).
- [6] F.-K. Thielemann, J.H. Applegate, J.J. Cowan, M. Wiescher, in *Nuclei in the Cosmos*, ed. H. Oberhummer (Springer, Berlin, 1991), p. 147.
- [7] T. Rauscher, J.H. Applegate, J.J. Cowan, F.-K. Thielemann, and M. Wiescher, *Ap. J.* **429**, 499 (1994).
- [8] W.E. Burcham and J.M. Freeman, *Philos. Mag.* **40**, 807 (1950); **41**, 337 (1950).
- [9] J. Szabó, J. Csikai, and M. Várnagy, *Nucl. Phys.* **A195**, 527 (1972).
- [10] G.C. Bach and D.J. Livesey, *Phil. Mag.* **46**, 824 (1955).
- [11] M. Wiescher, R.N. Boyd, S.L. Blatt, L.J. Rybarczyk, J.A. Spizuoco, R.E. Azuma, E.T.H. Clifford, J.D. King, J. Görres, C. Rolfs, and A. Vlieks, *Phys. Rev. C* **28**, 1431 (1983).
- [12] H. Bucka, P. Heide, F. Knape, *Verhandl. DPG (VI)* **27**, **1**, 128 (1992).
- [13] F. Knape, PhD thesis, Technical University Berlin, 1992; F. Knape, private communication.
- [14] C. Angulo, S. Engstler, G. Raimann, C. Rolfs, W.H. Schulte, and E. Somorjai, *Z. Phys. A*, *Z. Phys. A* **345**, 231 (1993).

- [15] C. Angulo, W.H. Schulte, D. Zahnow, G. Raimann, and C. Rolfs, *Z. Phys. A*, **345**, 333 (1993).
- [16] J.M. Davidson, H.L. Berg, M.M. Lowry, M.R. Dwarakanath, A.J. Sierk, and P. Batay-Csorba, *Nucl. Phys.* **A315**, 253 (1979).
- [17] H.W. Becker, C. Rolfs, and H.P. Trautvetter, *Z. Phys. A* **327**, 341 (1987).
- [18] T.A. Tombrello, in *Nuclear Research with Low Energy Accelerators*, eds. J.B. Marion and D.M. Van Patter (Academic Press, New York, 1967).
- [19] J.N. Bahcall, *Neutrino Astrophysics* (Cambridge University Press, Cambridge, 1989).
- [20] H. Oberhummer, H. Herndl, H. Leeb, and G. Staudt, *Kerntechnik* **53**, 211 (1989).
- [21] G. Raimann, B. Bach, K. Grün, H. Herndl, H. Oberhummer, S. Engstler, C. Rolfs, H. Abele, R. Neu, and G. Staudt, *Phys. Lett. B* **249**, 191 (1990).
- [22] H. Herndl, H. Abele, G. Staudt, B. Bach, K. Grün, H. Scsribany, H. Oberhummer, and G. Raimann, *Phys. Rev. C* **44**, R952 (1991).
- [23] H. Oberhummer and G. Staudt, in *Nuclei in the Cosmos*, ed. H. Oberhummer (Springer, Berlin, 1991), p. 29.
- [24] T. Rauscher, K. Grün, H. Krauss, H. Oberhummer, and E. Kwasniewicz, *Phys. Rev. C* **45**, 1996 (1992).
- [25] B. Bach, K. Grün, G. Raimann, and T. Rauscher, Technical University Vienna, Austria, computer code TETRA (unpublished).
- [26] G.R. Satchler, *Direct Nuclear Reactions* (Clarendon Press, Oxford, 1983).
- [27] N.K. Glendenning, *Direct Nuclear Reactions* (Academic Press, New York, 1983).
- [28] F. Hoyler, H. Oberhummer, T. Rohwer, G. Staudt, and H.V. Klapdor, *Phys. Rev. C* **31**, 17 (1985).

- [29] D. Kurath and D.J. Millener, Nucl. Phys. **A238**, 269 (1975).
- [30] G.R. Satchler and W.G. Love, Phys. Rep. **55**, 183 (1979).
- [31] A.M. Kobos, B.A. Brown, R. Lindsay, and G.R. Satchler, Nucl. Phys. **A425**, 205 (1984).
- [32] H. DeVries, C.W. DeJager, C. DeVries, At. Data and Nucl. Data Tabl. **36**, 495 (1987).
- [33] F. Ajzenberg-Selove, Nucl. Phys. **A506**, 1 (1990).
- [34] A.H. Wapstra and G. Audi, Nucl. Phys. **A432**, 1 (1985).
- [35] H.J. Hauser, M. Walz, F. Weng, G. Staudt, and P.K. Rath, Nucl. Phys. **A456**, 253 (1986).
- [36] G. Weber, PhD thesis, Technical University Berlin, 1989.
- [37] C.E. Rolfs and W.S. Rodney, *Cauldrons in the Cosmos* (University of Chicago Press, Chicago, 1988).
- [38] C. Rolfs, W.S. Rodney, Nucl. Phys. **A235**, 450 (1974).
- [39] W.A. Fowler, G.R. Caughlan, and B.A. Zimmerman, Ann. Rev. Astron. Astrophys. **13**, 69 (1975).
- [40] G.R. Caughlan and W.A. Fowler, At. Data Nucl. Data Tabl. **40**, 283 (1988).
- [41] J. Jaki, B.M. Barnett, H. Clement, W. Gyles, R.R. Johnson, Ch. Joram, W. Kluge, S. Krell, H. Matthäy, M. Metzler, D. Renker, R. Tacik, G.J. Wagner, C.A. Wiedner, and U. Wiedner, Phys. Lett. B **238**, 36 (1990).
- [42] W.B. Cottingham, K.G. Boyer, W.J. Braithwaite, S.J. Greene, C.J. Harvey, R.J. Joseph, D.B. Holtkamp, C. Fred Moore, J.J. Kraushaar, R.J. Peterson, R.A. Ristinen, J.R. Shepard, G.R. Smith, R.L. Boudrie, N.S.P. King, C.L. Morris, J. Piffaretti, and H.A. Thiessen, Phys. Rev. C **36**, 230 (1987).
- [43] H. Clement, private communication.

- [44] O. Schönfeld and G. Staudt, private communication.
- [45] C.M. Perey and F.G. Perey, *At. Data and Nucl. Data Tabl.* **17**, 1 (1976).
- [46] P. Wund and G. Staudt, private communication.
- [47] F. Ajzenberg-Selove, *Nucl. Phys.* **A490**, 1 (1988).

FIGURES

FIG. 1. S -factor data of the reaction $^{10}\text{B}(p,\alpha_0)^7\text{Be}$ in the range $E_{c.m.} \leq 0.04$ MeV. The curve is the result of the DWBA calculation. The experimental data are represented by triangles [14], and by squares [13].

FIG. 2. S -factor data of the reaction $^{10}\text{B}(p,\alpha_0)^7\text{Be}$ in the range $0.04 \leq E_{c.m.} \leq 0.15$ MeV. The curve is the result of the DWBA calculation. The experimental data are represented by triangles [14], and by squares [13].

FIG. 3. S -factor data of the reaction $^{10}\text{B}(p,\alpha_1)^7\text{Be}^*$ in the energy range $E_{c.m.} \leq 0.2$ MeV. The experimental data are taken from Ref. [15]. Shown are the DWBA contribution (dotted), the Breit-Wigner contribution (dashed) and the sum of DWBA, Breit-Wigner and interference term (solid).

FIG. 4. Ratio of the reaction rate of $^{10}\text{B}(p,\alpha)^7\text{Be}$ obtained in this work to rate values from Refs. [39,40].

FIG. 5. S -factor data of the reactions $^{11}\text{B}(p,\alpha_1)^8\text{Be}^*$ and $^{11}\text{B}(p,\alpha_0)^8\text{Be}$. Dashed curves: non-resonant contribution (DWBA); solid curves: contribution from the sum of DWBA, Breit-Wigner and interference terms. The data are taken from Refs. [17] (triangles) and [14] (circles).

TABLES

TABLE I. Spectroscopic factors for $^{10}\text{B} = \text{t} + ^7\text{Be}$.

$J(^7\text{Be})$	$E_x (^7\text{Be})^{\text{a}}$	$P_{3/2}$	$F_{5/2}$	$F_{7/2}$
1/2	1.1 MeV		0.0136	0.0037
3/2	0.0 MeV	0.0812	0.0706	0.2571

^a E_x is the excitation energy calculated from the shell model [29].

TABLE II. Parameters of the optical and bound state potentials for the reaction $^{10}\text{B}(\text{p},\alpha)^7\text{Be}$.

$\text{p} + ^{10}\text{B}$	Real part: single-folding potential $\lambda_p = 1.326$ $r_c = 1.2 \text{ fm}^{\text{a}}$ Imaginary part: Saxon-Woods derivative potential $W_D = -15 \text{ keV}$, $r_D = 1.5 \text{ fm}^{\text{a}}$, $a_D = 0.5 \text{ fm}^{\text{a}}$
$\alpha + ^7\text{Be}$	Real part: double-folding potential $\lambda_\alpha = 1.7$ $r_c = 1.69 \text{ fm}^{\text{a}}$ Imaginary part: Saxon-Woods volume potential $W_V = -4.6 \text{ MeV}$, $r_V = 1.4 \text{ fm}^{\text{a}}$, $a_V = 0.52 \text{ fm}^{\text{a}}$
Bound state ($\text{t} + ^7\text{Be}$)	double-folding potential λ^{b} $r_c = 1.4 \text{ fm}^{\text{a}}$

^aTaken from Ref. [45].

^bCalculated for the different separation energies corresponding to the different states of ^7Be [47] (see text for more information).

TABLE III. Spectroscopic factors for $^{11}\text{B} = \text{t} + ^8\text{Be}$.

$J(^8\text{Be})$	$E_x (^8\text{Be})^{\text{a}}$	$\text{P}_{1/2}$	$\text{P}_{3/2}$	$\text{F}_{5/2}$	$\text{F}_{7/2}$
0	0.0 MeV		0.2632		
2	3.4 MeV	0.0001	0.4669	0.0618	0.0577

^a E_x is the excitation energy calculated from the shell model [29].

TABLE IV. Parameters of the optical and bound state potentials for the reaction $^{11}\text{B}(p,\alpha)^8\text{Be}$.

$p + ^{11}\text{B}$	Real part: single-folding potential $\lambda_p = 0.81$ $r_c = 1.29 \text{ fm}^a$
$\alpha + ^8\text{Be}$	Real part: double-folding potential $\lambda_\alpha = 1.21$ $r_c = 1.55 \text{ fm}^{ab}$ Imaginary part: Saxon-Woods volume potential $W_V = -3 \text{ MeV}$, $r_V = 1.75 \text{ fm}^{ab}$, $a_V = 0.65 \text{ fm}^{ab}$
Bound state $(t + ^8\text{Be})$	double-folding potential λ^c $r_c = 1.5 \text{ fm}^{ab}$

^aTaken from Ref. [45].

^bAveraged (see text).

^cCalculated for the different separation energies corresponding to the different states of ^8Be [47] (see text for more information).

TABLE V. Results of the Breit-Wigner fits for the reaction $^{11}\text{B}(p,\alpha)^8\text{Be}$.

Reaction	Resonance 1	Resonance 2
$^{11}\text{B}(p,\alpha_0)^8\text{Be}$	$\theta_p^2 = 0.017$ $\Gamma_\alpha = 5.5 \text{ keV}$	
$^{11}\text{B}(p,\alpha_1)^8\text{Be}^*$	$\theta_p^2 = 0.570$ $\Gamma_\alpha = 5.7 \text{ keV}$ $E_{c.m.} = 148.5 \text{ keV}^a$	$\theta_p^2 = 0.604$ $\Gamma_\alpha = 296.5 \text{ keV}$ $E_{c.m.} = 660 \text{ keV}$

^aNo fit parameter; value was taken from Ref. [33].

TABLE VI. Reaction rate $N_A \langle \sigma v \rangle$ of the reaction $^{10}\text{B}(p,\alpha)^7\text{Be}$ in $\text{cm}^3\text{s}^{-1}\text{mole}^{-1}$. The rate calculated with DWBA for bare nuclei is compared to values given in previous work.

Temperature ^a	Caughlan <i>et al.</i> ^b	Youn <i>et al.</i> ^c	this work
0.002	0.209×10^{-28}		0.494×10^{-26}
0.004	0.496×10^{-20}		0.175×10^{-17}
0.006	0.561×10^{-16}		0.208×10^{-13}
0.008	0.200×10^{-13}		0.630×10^{-11}
0.010	0.129×10^{-11}	0.167×10^{-9}	0.323×10^{-9}
0.012	0.310×10^{-10}	0.319×10^{-8}	0.607×10^{-8}
0.014	0.391×10^{-9}	0.326×10^{-7}	0.605×10^{-7}
0.016	0.315×10^{-8}	0.217×10^{-6}	0.393×10^{-6}
0.018	0.184×10^{-7}	0.107×10^{-5}	0.188×10^{-5}
0.020	0.836×10^{-7}	0.416×10^{-5}	0.716×10^{-5}
0.025	0.173×10^{-5}	0.617×10^{-4}	0.102×10^{-3}
0.030	0.174×10^{-4}	0.471×10^{-3}	0.754×10^{-3}
0.035	0.109×10^{-3}		0.369×10^{-2}
0.040	0.495×10^{-3}	0.880×10^{-2}	0.136×10^{-1}
0.045	0.177×10^{-2}		0.406×10^{-1}
0.050	0.530×10^{-2}	0.687×10^{-1}	0.104×10^0
0.060	0.321×10^{-1}	0.324×10^0	0.484×10^0
0.070	0.135×10^0	0.110×10^1	0.164×10^1
0.080	0.437×10^0	0.301×10^1	0.448×10^1
0.090	0.118×10^1	0.700×10^1	0.104×10^2
0.100	0.277×10^1	0.144×10^2	0.214×10^2
0.120	0.112×10^2	0.468×10^2	0.700×10^2
0.140	0.341×10^2	0.119×10^3	0.179×10^3
0.160	0.850×10^2	0.254×10^3	0.387×10^3

0.180	0.183×10^3	0.481×10^3	0.739×10^3
0.200	0.354×10^3	0.831×10^3	0.129×10^4
0.300	0.355×10^4	0.552×10^4	0.899×10^4
0.400	0.149×10^5	0.179×10^5	0.302×10^5
0.500	0.412×10^5	0.415×10^5	0.707×10^5
0.600	0.891×10^5	0.814×10^5	0.134×10^6
0.700	0.165×10^6	0.145×10^6	0.219×10^6
0.800	0.276×10^6	0.240×10^6	0.324×10^6
0.900	0.430×10^6	0.379×10^6	0.442×10^6
1.000	0.634×10^6	0.571×10^6	0.570×10^6

^aGiven in 10^9 K.

^bCalculated with the parametrization given in Refs. [39,40].

^cHere we cite Ref. [4].

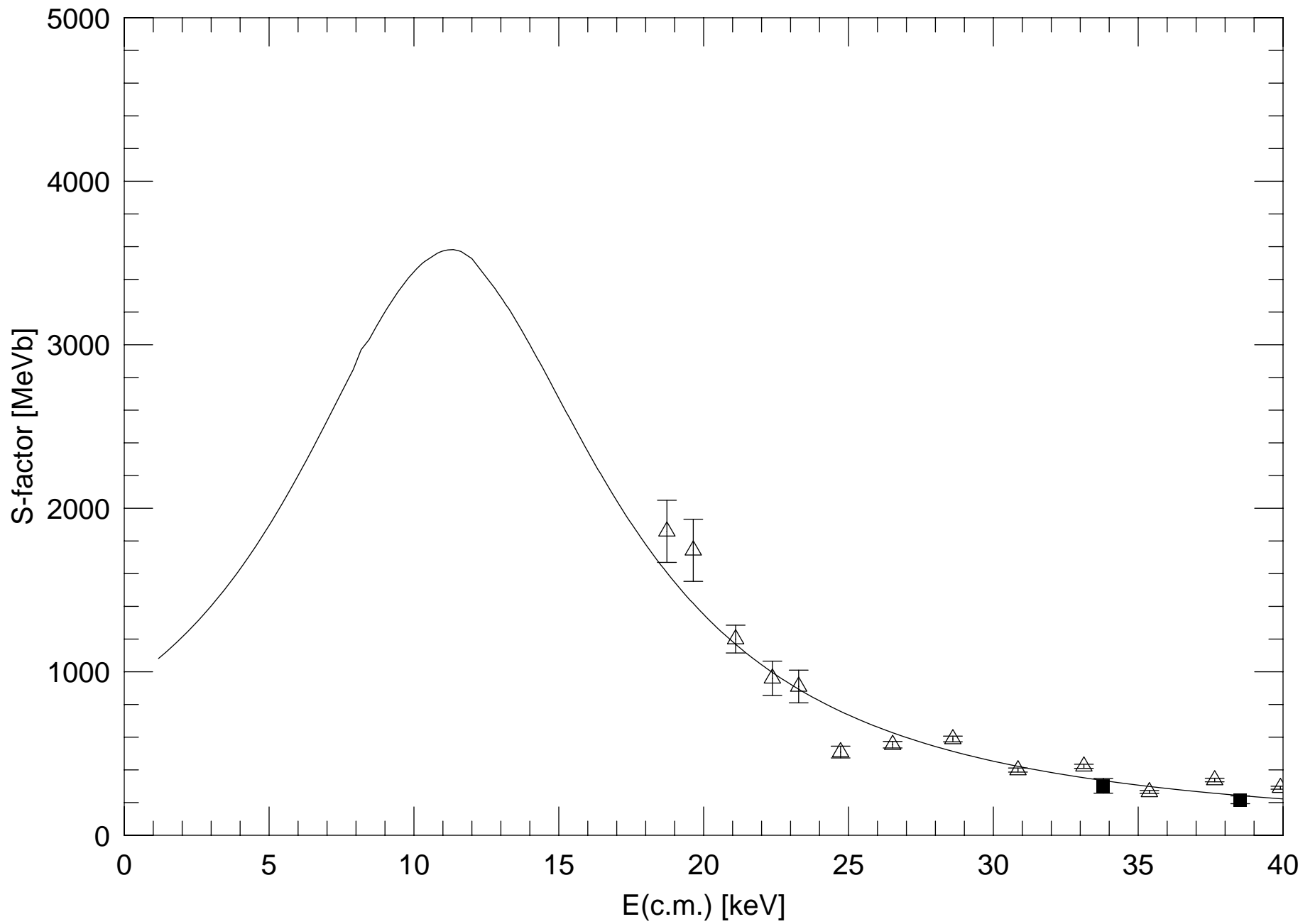
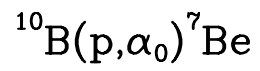
TABLE VII. Reaction rates $N_A \langle \sigma v \rangle$ of the reaction $^{11}\text{B}(p,\alpha)^8\text{Be}^*$ in $\text{cm}^3\text{s}^{-1}\text{mole}^{-1}$. The rate calculated with DWBA is compared to values given in previous work.

Temperature ^a	Caughlan <i>et al.</i> ^b	this work
0.002	0.284×10^{-27}	0.197×10^{-31}
0.004	0.715×10^{-19}	0.281×10^{-19}
0.006	0.834×10^{-15}	0.613×10^{-15}
0.008	0.303×10^{-12}	0.383×10^{-12}
0.010	0.200×10^{-10}	0.255×10^{-10}
0.012	0.486×10^{-9}	0.563×10^{-9}
0.014	0.618×10^{-8}	0.702×10^{-8}
0.016	0.504×10^{-7}	0.582×10^{-7}
0.018	0.296×10^{-6}	0.349×10^{-6}
0.020	0.136×10^{-5}	0.162×10^{-5}
0.025	0.286×10^{-4}	0.345×10^{-4}
0.030	0.291×10^{-3}	0.353×10^{-3}
0.035	0.185×10^{-2}	0.226×10^{-2}
0.040	0.849×10^{-2}	0.104×10^{-1}
0.045	0.307×10^{-1}	0.377×10^{-1}
0.050	0.927×10^{-1}	0.114×10^0
0.060	0.571×10^0	0.708×10^0
0.070	0.244×10^1	0.304×10^1
0.080	0.808×10^1	0.102×10^2
0.090	0.226×10^2	0.286×10^2
0.100	0.558×10^2	0.711×10^2
0.120	0.267×10^3	0.339×10^3
0.140	0.990×10^3	0.123×10^4
0.160	0.293×10^4	0.358×10^4

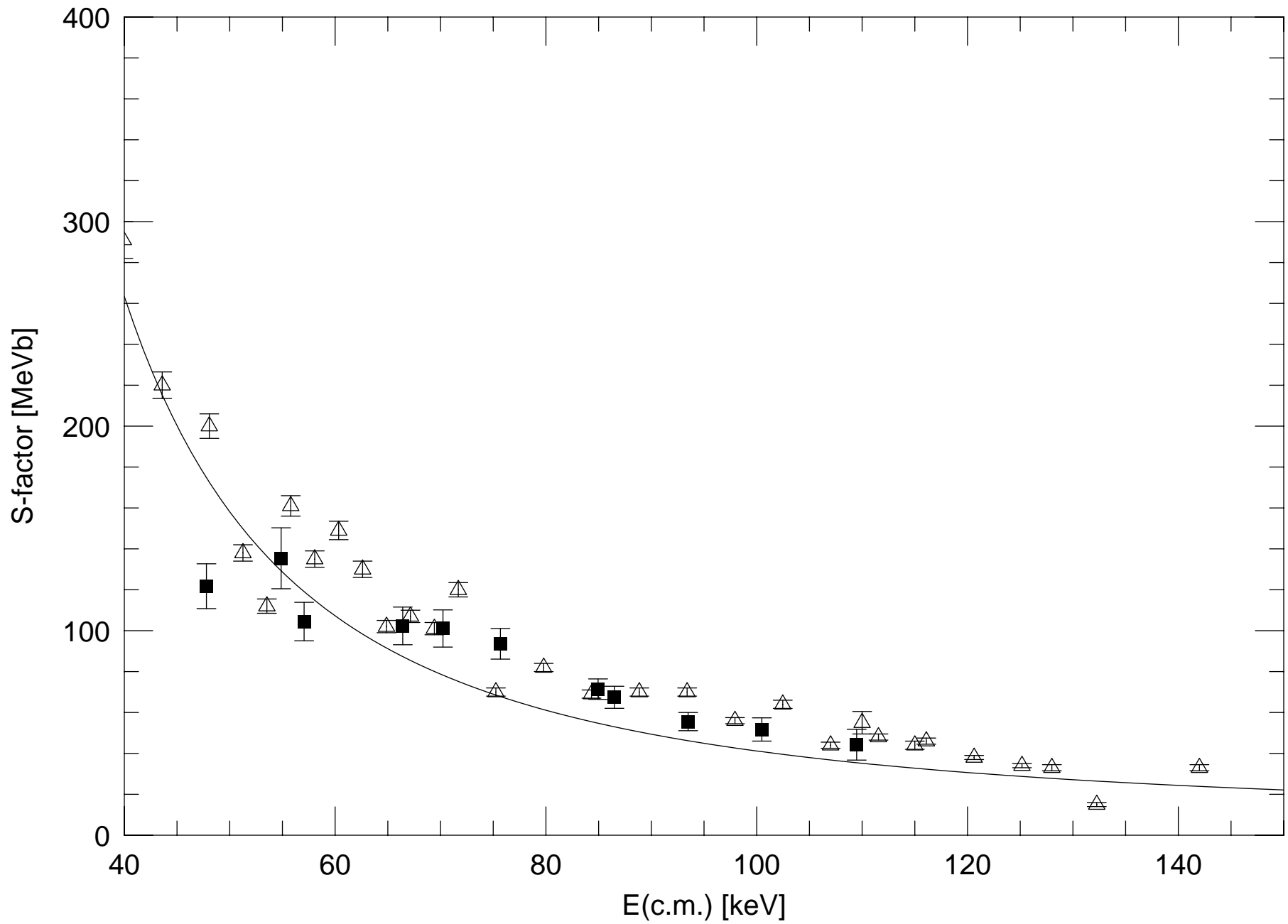
0.180	0.717×10^4	0.864×10^4
0.200	0.150×10^5	0.180×10^5
0.300	0.153×10^6	0.187×10^6
0.400	0.552×10^6	0.711×10^6
0.500	0.138×10^7	0.183×10^7
0.600	0.298×10^7	0.381×10^7
0.700	0.588×10^7	0.689×10^7
0.800	0.106×10^8	0.112×10^8
0.900	0.174×10^8	0.167×10^8
1.000	0.264×10^8	0.233×10^8

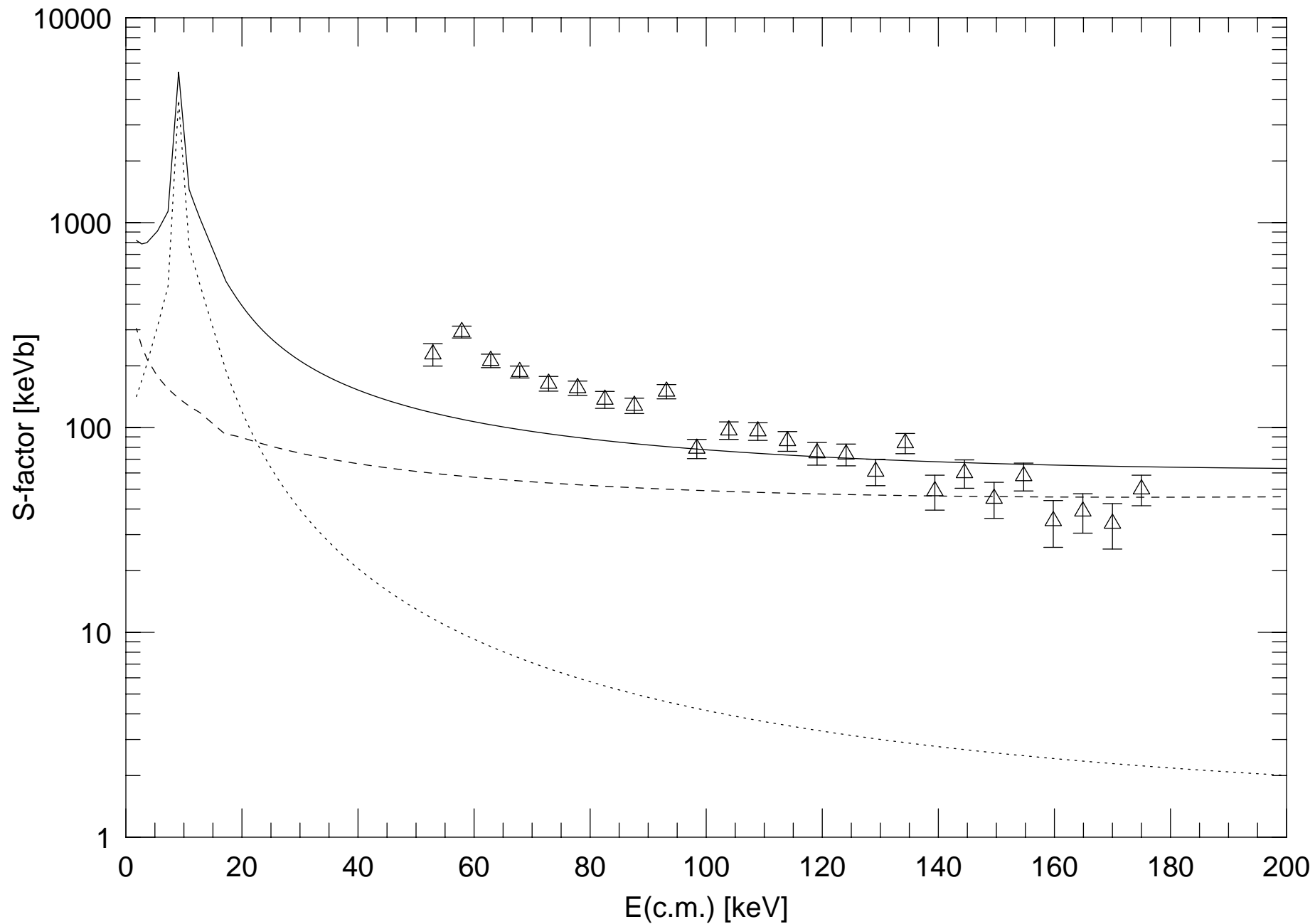
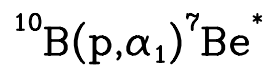
^aGiven in 10^9 K.

^bHere we cite Ref. [40].



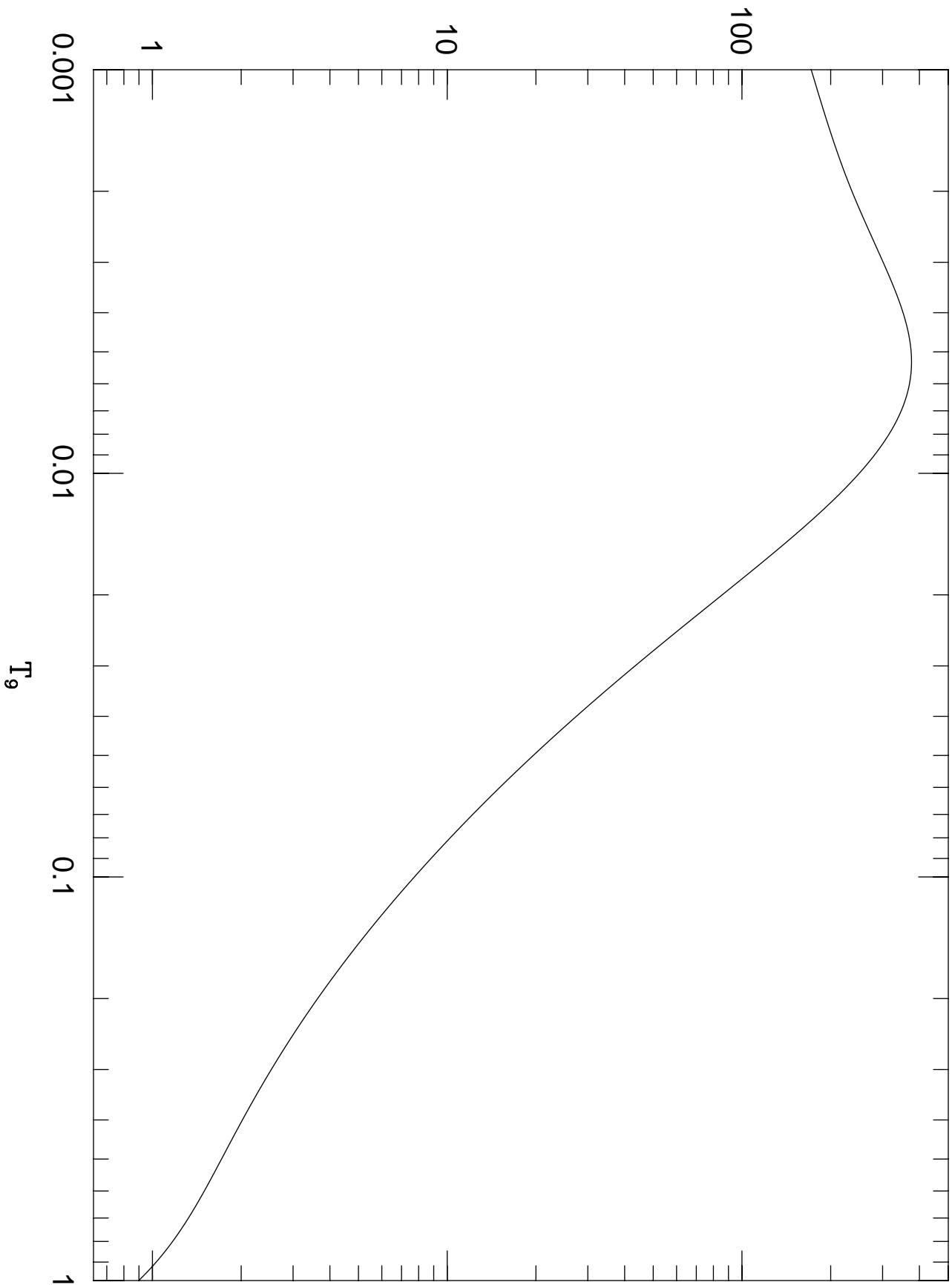
$^{10}\text{B}(p,\alpha_0)^7\text{Be}$





Ratio of Reaction Rates

$^{10}\text{B}(p,\alpha)^7\text{Be}$



$^{11}\text{B}(p,\alpha)^8\text{Be}$ 